Chemistry—Methods

Research Article
doi.org/10.1002/cmtd.202300043

Chemistry Europe
European Chemical Societies Publishing

www.chemistrymethods.org

pHbot: Self-Driven Robot for pH Adjustment of Viscous Formulations via Physics-informed-ML**

Aniket Chitre[+],[a, b, c] Jayce Cheng[+],[c] Sarfaraz Ahamed,[c, d] Robert C. M. Querimit,[c, e] Benchuan Zhu,[f] Ke Wang,[f] Long Wang,[f] Kedar Hippalgaonkar,*[c, d] and Alexei A. Lapkin*[a, b]

pH adjustment is crucial for many industrial products, yet this step is typically performed by manual trial-and-error. A particularly industrially relevant yet challenging titration is that of adjusting viscous liquid formulations using weak, polyprotic titrants (usually citric acid). Handling of viscous, non-Newtonian formulations, with such polyprotic acids preferred for their chelation and buffering effects make a robotic solution challenging. We present a self-driving pH robot integrated with physics-informed learning; this hybrid physical-ML model enables automated titration with weak-strong acid/base pairs. To deal with the high viscosities of these formulations, we developed specific automated mixing and cleaning protocols. We hit the target pH within two to five iterations over 250 distinct formulations in lab-scale small-batch (~10 mL and 12 samples) titrations. In the interest of scaling up to match industrial processes, we also demonstrate that our hybrid algorithm works at ~25× scale-up. The method is general, and we open-source our algorithm and designs.

Introduction

pH adjustment is important across several product development processes, including in the formulations, pharmaceutical manufacturing, and the food and beverage industries.[1–7] The pH can affect the functionality, performance, and safety of the product. Our study focuses on the industrially motivated problem statement to titrate a wide range of consumer care formulations at the research and development (R&D) scale where a large number of products are tested. This work forms part of a broader study developing a high-throughput shampoo formulations dataset and pH adjustment is a key processing step. Manufacturers typically adjust shampoo to between pH 5.5–7 to prevent scalp irritation (from lower pHs) and shampoos are non-alkaline to prevent cuticle damage and frizzy hair.[3,4] pH adjustment is currently performed manually by a trained lab chemist who adds the acid or base in a dropwise fashion until the pH target is met. This is slow and inefficient; therefore, an automated and predictive pH adjustment method is required.

In principle, the pH can be lowered with any acid, however, industrially many consumer care formulations, including shampoo, are adjusted with citric acid[8–10] Citric acid ($H_3C_6H_5O_7$) is preferred as it can contribute chelating effects and buffering properties to cosmetics and personal care products.[8] This is because it is a weak, polyprotic acid; however, it is exactly these properties which simultaneously make it a challenging titrant to work with. Unlike strong acids, citric acid's deprotonation state (where pH is defined as the negative log decade of the solution's proton, i.e., H_3O^+, concentration) is pH-dependent. Therefore, we cannot straightforwardly determine how much citric acid needs to be added to lower the pH appropriately. When developing new formulations in R&D we wish to screen many different products; hence, the analyte's chemical properties, for example, acid or base hydrolysis constants (K_a/K_b) are

[a] A. Chitre,[+] Prof. A. A. Lapkin
Department of Chemical Engineering and Biotechnology
University of Cambridge
Philippa Fawcett Drive
Cambridge CB3 0AS (UK)
E-mail: aal35@cam.ac.uk

[b] A. Chitre,[+] Prof. A. A. Lapkin
Cambridge Centre for Advanced Research and Education in Singapore
CARES Ltd. 1 CREATE Way, CREATE Tower #05-05
Singapore 138602 (Singapore)

[c] A. Chitre,[+] Dr. J. Cheng,[+] S. Ahamed, R. C. M. Querimit, Prof. K. Hippalgaonkar
Institute of Materials Research and Engineering
Agency for Science, Technology and Research (A*STAR)
Singapore 138634 (Singapore)
E-mail: kedar@ntu.edu.sg

[d] S. Ahamed, Prof. K. Hippalgaonkar
Department of Materials Science and Engineering
Nanyang Technological University
Singapore, 117575 (Singapore)

[e] R. C. M. Querimit
School of Chemistry
Chemical Engineering and Biotechnology
Nanyang Technological University
Singapore 637459 (Singapore)

[f] Dr. B. Zhu, Dr. K. Wang, Dr. L. Wang
BASF Advanced Chemicals Co. Ltd.
No. 300, Jiang Xin Sha Road
Pudong, Shanghai 200137 (China)

[+] These authors have contributed equally.

[**] A previous version of this manuscript has been deposited on a preprint server (https://doi.org/10.26434/chemrxiv-2023-c46mv).

Supporting information for this article is available on the WWW under https://doi.org/10.1002/cmtd.202300043

not typically known, especially as these products are complex mixtures. Therefore, we cannot use a method such as the Henderson-Hasselbalch (HH) equation to model the pH change effected by an addition of acid or base. Furthermore, HH has limited applicability to polyprotic buffer systems.[11,12] Unlike production level processes where the product properties are well known, we need a titration process agnostic to the product's chemistry at the R&D stage. One strategy is to use proportional, integral, derivative (PID) control, however, such a method is not predictive without the implementation of more complex model-based control algorithms. Here we show the utility of machine learning based methods for pH adjustment.

A solution method was introduced recently: a Gaussian Process (GP) model is trained on the net volume of acid (−) or base (+) added.[13] Efficiency of this target optimisation method was ensured by including the *a priori* known shape of a titration curve, which is chemistry-specific to the sample to be titrated, into the GP via artificial datapoints (taking a point each with lower pH and more acid and the vice versa for base, relative to the initial datapoints). The convention followed is that the addition of acid is negative and base positive. The same convention is used in this study. While this solution is effective in titration of unknown formulations with hydrochloric acid (HCl) and sodium hydroxide (NaOH), the published method is limited to systems that do not generate buffers upon titration.

In this study, we address a more general problem of pH adjustment, where a formulation that could be quite viscous and whose composition is unknown is being titrated by a weak acid or sodium hydroxide to a target pH of 5.8±0.2, as set by our industrial partner. This more general problem is more complex. Firstly, there is no longer equivalent stoichiometry between the protons/hydroxide ions released by the acid/base pair and the "strength", the amount of protons released into the solution, by citric acid is pH-dependent. Secondly, if there is an overshoot, a correction will result in a citrate buffer system being formed, which will make the product being titrated resistant to pH change, severely complicating the titration. In manual titrations, the overshot titration samples are frequently abandoned, and the titration is attempted afresh. Hence, for this reason, the initial sampling strategy to randomly select three initial data points to start developing a statistical model, as shown in,[13] is unsuitable. And finally, variable viscosity of samples requires adjustment of the titration procedure to ensure measurements are done at correct times.

In this work we developed a hybrid "physics-informed" ML strategy to successfully adjust the pH of liquid formulations with citric acid/sodium hydroxide by incorporating the knowledge from the physical chemistry of the titrants. For example, we calculate and use the speciation state for the weak, polyprotic titrant to better predict how much acid/base to dose and additionally, the capacity of these titrants to generate a buffer system informed our development of a multi-stage titration algorithm. This algorithm generalises to other strong-strong or weak-strong titrant pairs.

Secondly, we address the engineering challenge of high-throughput pH adjustment of potentially viscous formulations. In the spirit of the "Fourth Industrial Revolution" and digitalisation of formulations research and development (R&D), the pH adjustment would ideally be fully automated.[14–16] A simple automated pH adjustment system was shown in,[13] however, it cannot cope with viscous samples. Without sufficient mixing after addition of acid or base, pH will not reach its true equilibrium value and experimental measurements may be erroneous if recorded too soon. In addition, without the ability to clean a pH probe from viscous residues of the sample materials it would be impossible to automate a batch of titrations as manual cleaning would be required in between samples. To the best of our knowledge, there is no suitable automated titration system on the market and thus, we present and open-source such an autonomous platform suitable for viscous formulations.

Results and Discussion

We present a computer rendering of the developed titration robot in Figure 1a and a video of operation in the Supporting Information. The robot has a design that facilitates autonomous, closed-loop pH adjustment for small-scale (~10 mL) batches of up to 12 samples. We first discuss the design of the pH robot, followed by the "physics-informed" multi-stage titration algorithm developed in this study. Figure 1b shows the statistical model that we fit over the net moles of H_3O^+ or OH^- ions. We calculate the input space for this titration curve by considering the pH-dependent speciation state of the weak acid used in the titration, as shown in Figure 1c. We further explain this in the sub-section describing the incorporation of the titrants' physical chemistry into the ML feature space. The titration algorithm is adaptive to whether we are: (i) initially sampling, (ii) in the main phase of titration, or (iii) applying a correction for overshooting the set point – separate sub-sections are presented on each stage. We utilise the pH robot to titrate a large range of samples, and we present illustrative examples and evaluate the efficiency of the titration algorithm. Finally, we demonstrate the method is generalisable to volumes closer to industrial formulation development tasks.

Design and Development of the pH Robot

Objected-oriented hardware design is a powerful heuristic for matching high-throughput laboratory equipment with experiment workflows by remaining initially tool-agnostic during workflow layout, but subsequently building or incorporating automated tools to fit the workflow, which evolves according to design concerns.[17] We commenced workflow layout by first elucidating a generic titration process that would typically be performed manually, shown in Figure 2, with the addition of ML in-the-loop to account for the future self-driving capability of this platform. The workflow, beginning with analyte input and ending with labware cleaning, is the unit operation of this self-driving platform, i.e., the operation that will be repeated in an automated fashion. At this point, any arbitrary titration work-

Research Article
doi.org/10.1002/cmtd.202300043
Chemistry Europe
European Chemical Societies Publishing

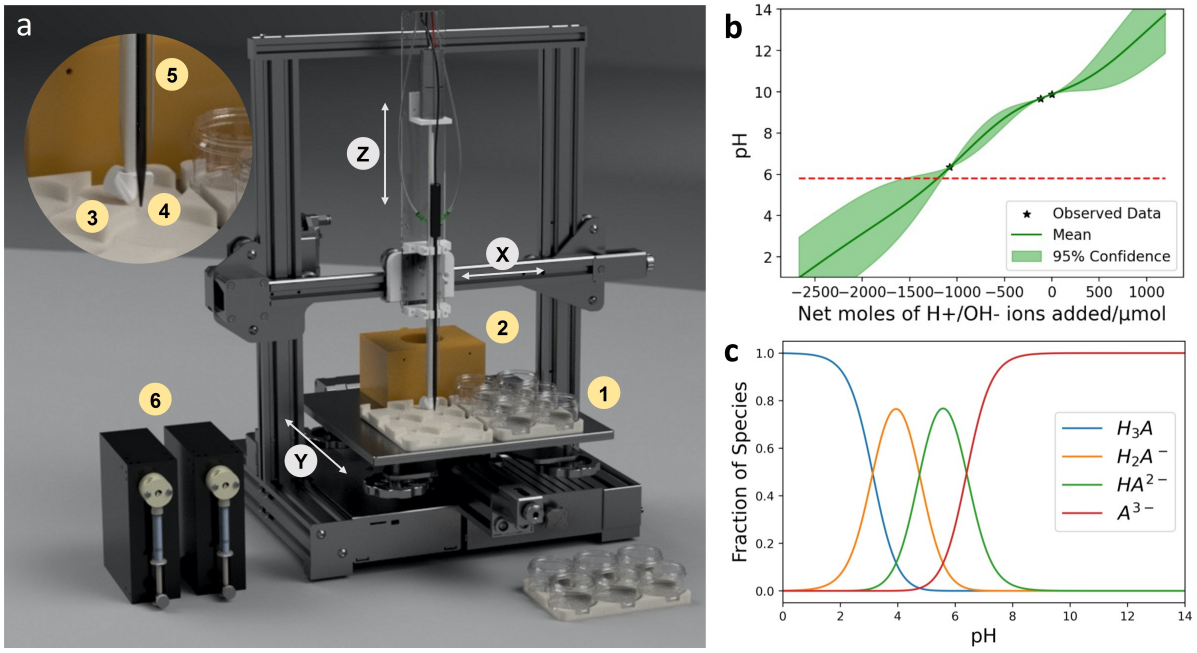

Figure 1. a) A computer image of the developed robotic titration platform. This specific configuration includes: (1) customised labware with MTP-standard dimensions as sample container holders on the 3D printer stage. The rear of the Y-translating stage also supports a customised IPA wash station (2). The X–Z-translating probe head (inset, magnified) incorporates a high-torque mechanical stirrer (3), (4) a slim profile pH probe and (5) two dispensing syringe needles for the acid and base. The needles are coupled to syringe pumps (6). The entire assembly is controlled in a Python IDE via serial communication to achieve self-driving capability. b) A "physics-informed" machine learning (ML) method is used to drive closed-loop optimisation towards the target pH (red dashed line). c) The speciation diagram, here modelled for citric acid ($A = C_6H_5O_7$), is used to calculate the effective strength of the acid added.

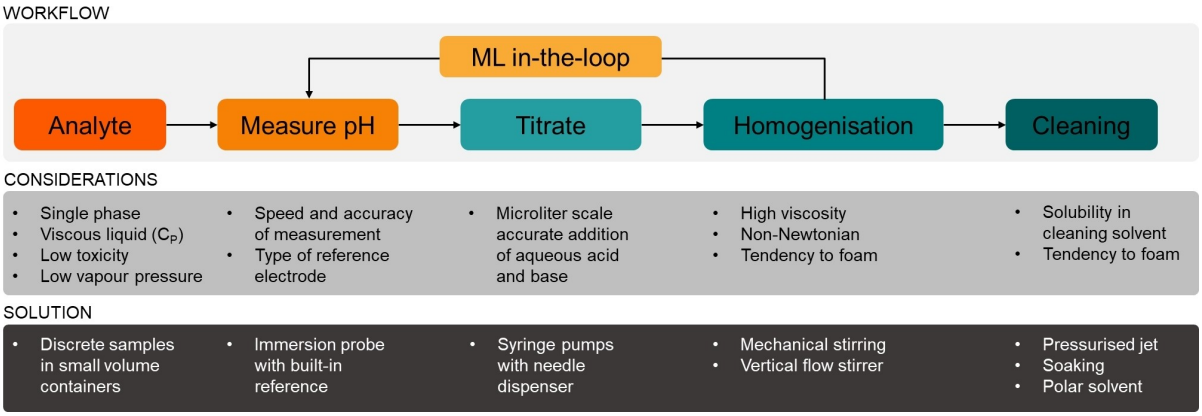

Figure 2. Schematic of hardware design process guided by experimental workflow and sample considerations.

flow can be mapped onto our system, regardless of chemistry, viscoelastic properties, etc.

We then list the characteristics of each workflow step that are unique to our experiment. As can be seen in Figure 2, each step of automating the titration process involves considerations related to material properties (e.g., viscosity, polarity, surface tension) as well as equipment limitations (e.g., speed, accuracy, and precision). Our analyte can be a non-Newtonian liquid with an apparent viscosity of up to 5000 cP based on the experimentally measured rheology upper bound for formulated products successfully titrated on the pHbot. After excluding unstable formulations in pre-screening, we know our analytes to be single-phase solutions. Being consumer care products, they also have low toxicity and low vapour pressure, obviating the need for exhaust systems for experiments carried out in this article; the system is compact enough to be located within a fume hood for working with chemicals with more stringent exposure levels.

While our methods are generally applicable, our focus is solving the harder challenge of high viscosity and non-Newtonian behaviour of the analyte, which will be our principal consideration, i.e., this material parameter is likely to have an impact on design choices for almost all steps of the workflow. The addition of aqueous titrant to a viscous analyte requires a homogenisation technique that can generate high shear rates and induces convective flow that collects material from the

edges of the container. Finally, the complete removal of reactants that have come into contact with parts of the titration platform between unit operations is critical for minimising cross-contamination between samples – highly viscous samples likely require chemo-mechanical techniques for effective cleaning.

Identifying the principal consideration for this workflow lets us make more informed design choices by excluding hardware choices incapable of satisfying the needs of our experiment. To choose the overall experimental format, we first considered various methods of experimentally carrying out a titration. Titration is the process of determining the unknown concentration of one species by adjusting its molar ratio relative to another species of known concentration.[18] The *endpoint* is defined when a specific ratio between the two species is reached and can be analytically detected by a change in material property such as optical scattering (colorimetric, precipitation), electrochemical potential (potentiometric), enthalpy (calorimetric), etc.

Performing titrations swiftly and accurately can be achieved in several different ways. Continuous single-batch titration is the traditional, manual approach where titrant, held in a dispensing tool with high volumetric accuracy such as a burette, is continuously added to a test solution containing the analyte. The cumulative volume of titrant added at the endpoint yields the concentration of the analyte. This process is single-batch because each successive ratio of titrant:analyte exists in the same volume – unique ratios are separated temporally but not spatially. The flow analogue of this experiment is flow injection titration.[19,20] Separating samples spatially can be achieved in discrete batch titration, where each sample container holds a different ratio of titrant:analyte. The advantage of this technique is that the characterisation of the endpoint is generally less dependent on the speed of measurement. A second advantage is that throughput of discrete batch titration can be increased by using a discrete flow titration, where each unique ratio is continuously generated, typically by syringe pumps, and the endpoint is detected inline.[21,22]

Our design process is detailed in the decision tree shown in Figure 3. The high viscosity of our analyte precluded the use of discrete flow titration due to its tendency to clog and the difficulty of completely removing residue from tubing walls between discrete flow units. Discrete batch titration was also challenging to implement since both acidic and basic titrants were used – the large parameter space meant that generating discrete samples would be too time-consuming. The overall technique implemented was continuous, single-batch titration on individual samples.

Subsequently, we organised the computer numerical control (CNC) movement scheme for relative translation between samples and sensing/actuating elements. Individual samples of up to 15 mL were contained within jars that were organised into arrays conforming to MTP-format dimensions using custom 3D-printed holders. In the interest of compactness, we aggregated sensing and actuating elements into a single probe head that would concurrently perform liquid dispensing, pH measurement and homogenisation, as required by the experiment. Since translating and immersing the probe head between samples is a low agility-high accuracy (LA-HA) action, a Cartesian movement platform, as opposed to an articulated robot arm, was the obvious choice for achieving effective movement, while saving cost and time in implementation.[23–25] To maximise travel, a hybrid movement platform was used: the probe head translates in X–Z and the sample holding stage translates in Y. Here, the high viscosity of the analyte played to our advantage since samples could be moved quickly without spilling. The stage translation speed (Y-axis) can easily be controlled via the Python interface, and should be lowered, with corresponding reduction in throughput, for samples that might spill.

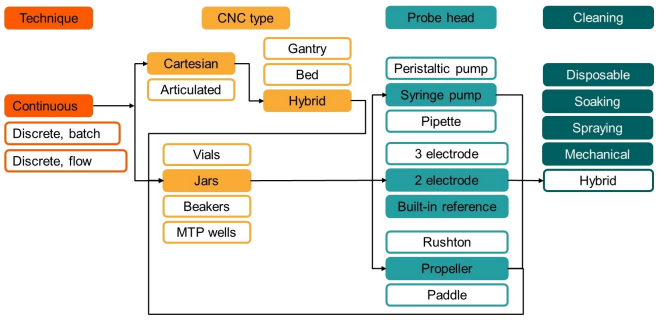

Figure 3. A decision tree for each design choice made during the Object-Oriented hardware harmonisation process. The highlighted boxes show the final choices made for each step of hardware design, keeping in consideration the requirements of the viscous mixing and titration – continuous single-batch titration performed with cartesian movement platform, jars to hold the analyte, syringe pumps to inject the titrants and slim probe pH head with propeller-based mixing and chemo-mechanical cleaning process.

The task of dispensing a titrant is characterised by high volumetric accuracy and small volumes. At the two extremes of liquid handling lie pipettes and continuous pumps: in pipettes, the volume to be dispensed is discrete for each operation, while in pumps the volume is continuously dispensed and measured temporally, or also gravimetrically. Both are capable of high accuracy. Syringe pumps equipped with multi-source valves offer a good compromise since volumes are measured with a reciprocating piston, but the multi-source valve allows different reactants to be aspirated/dispensed with the same syringe in a semi-continuous fashion. We opted for multi-source syringe pumps (TriContinent C3000) so that titrant tubes could be rinsed, if necessary. After dispensing acid/base, pH measurements were performed with a slim profile pH probe (Sentron MicroFET). Its two-electrode design and built-in reference performed well with test samples and was easily incorporated into the probe head.

Complete homogenisation of the titrant/analyte mixture was challenging due to their difference in viscosity and the large surface/volume ratio of the small sample containers. To mix aqueous titrant and a viscous reactant, our impeller needed to achieve high shear rates. We first tested a six-bladed Rushton turbine, which performed satisfactorily but was unable to collect viscous material from the sides and bottom of the sample container. This was to be expected since Rushton

turbines are characterised by high shear rate and a radial flow pattern. We fabricated a propeller mixer that would also generate an axial flow within the jars due to its ability to move liquid in the z-axis direction. We observed much shorter pH stabilisation times with the propeller mixer, confirming that complete homogenisation had taken place more quickly than with the Rushton turbine despite the lower shear rate. The propeller mixer was coupled to a high-torque DC gearmotor that was controlled with a pulse-width modulation (PWM) driver allowing speed and direction control.

Cleaning and waste management are oft-overlooked parts of the high-throughput experiment design process.[23] This belies their utmost importance: ensuring that labware, chemicals, and instruments are contamination-free – to levels that meet experimental demands – takes up an inordinate amount of time in any traditional laboratory and thus must be given careful consideration in an automated setup if we are to trust the generated data. As mentioned above, the high viscosity reactant made our task very challenging. Using disposable labware is convenient, but while the sample containers are indeed single-use, it was not possible to make the mixer and pH probe disposable.

For comprehensive removal of even trace organic residues, we turned to semiconductor photolithographic cleaning processes: the venerable "RCA clean" performs mechanical degreasing by ultrasonic-induced cavitation in increasingly polar solvents, namely trichloroethylene (TCE), acetone, isopropyl alcohol (IPA), and aqueous-based solutions.[26] We began by choosing an appropriate solvent from these – water-based cleaners were excluded since surfactants in the analyte would rapidly cause uncontrollable foaming. We sought a semi-polar solvent and conveniently found this in isopropyl alcohol (IPA) with a polarity index of 3.9 vs. 10.2 for water. We found that reactant residues soaked in IPA swelled upon immersion, while agitating the residues did not cause foaming. Since cleaning generates large amounts of chemical waste, the low toxicity and ease of disposal also made IPA a good choice as the cleaning agent. As shown in Figure 1a, we positioned our IPA cleaning bath at the rear of the stage such that it could be refilled easily. To avoid dripping residue while translating the probe head, we programmed movements to the cleaning bath along designed tracks that would not cross over the adjacent sample containers.

We found that while soaking the residues caused them to swell, they still adhered strongly to the propeller and the pH probe. Rotating the propeller while translating the probe head in the IPA bath was also ineffective. We discarded the idea of using mechanical brushes to scrub the propeller and the probe because the brushes would have to be cleaned or replaced, adding unnecessary processes. Brushes would also risk cross-contamination between runs. We achieved mechanical cleaning instead by using pressurised jets to dislodge residues. As shown in Figure 4, we fabricated a cleaning bath lid with a toroidal internal channel opening into a circular array of 1 mm cavities. When solvent is pumped into the channel with a diaphragm pump, the circular array directs pressurised jets of solvent onto the propeller and pH probe.

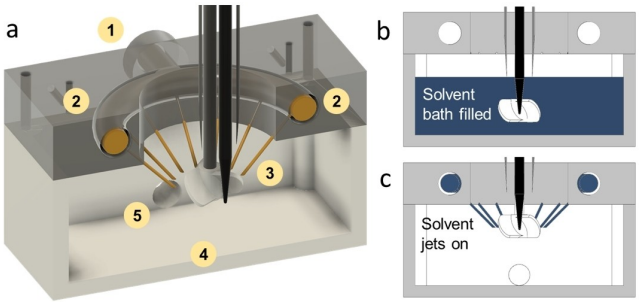

Figure 4. (a) Chemo-mechanical wash station cut-out schematic consisting of a top cover incorporating a solvent jet wash and bottom solvent bath. Pressurised solvent (colourised yellow for clarity) is pumped into the inlet (1) linked to a toroidal channel (2). A concentric array of 1 mm diameter openings in the channel (3) causes the solvent to spray onto the propeller and the pH probe head. The solvent collects in the base (4) where it fills a bath for submerging the propeller and probe. The outlet (5) is drained by a second pump allowing us to control the solvent level in the bath. (b) Immersing the propeller and probe in the filled solvent bath first loosens analyte residues by swelling before (c) the propeller and probe are raised to the confluence of the solvent jets for mechanical cleaning.

Our final hybrid cleaning approach implements chemo-mechanical cleaning as shown in Figure 4. The propeller and pH probe are first immersed in the solvent bath at the base of the wash station. This causes residues to swell and lose their mechanical integrity. Subsequently, the propeller and pH probes are raised to the level of the pressurised jets where the softened residues are mechanically dislodged. The propeller is rotated at full speed during washing, adding shear forces for improved cleaning. We found that the wash station was able to eliminate all traces of residue from the probe head for the range of formulation viscosities used in this experiment. Full control of washing parameters is achieved with two diaphragm pumps with speed controlled by PWM. The inlet pump regulates the jet pressure, while the outlet pump controls the solvent level in the bath by varying the solvent drain rate. Varying these two flow rates allows us to switch between soaking, spraying, and drainage modes with minimal actuation, reducing control complexity. Finally, the non-contact washing process means that no parts of the wash station are in physical contact with the probe head and thus the wash station is self-cleaning during the course of the experiment. Successfully implementing thorough washing of the probe head was integral to the self-driving nature of this platform, enabling fully automated titration. As IPA is a volatile liquid with a flash point of 12 °C and lower flammability limit (LFL) of just 2 v/v% (ThermoFischer), we were particularly concerned with releasing flammable IPA vapours. Therefore, it was ensured that the mounting piece for the pH probe and dosing needles completely covered the opening of the chemo-mechanical wash station whilst in operation and that the outlet pump was used to fully drain the wash station at the end of the washing cycle, so sufficient flammable vapours to reach the LFL could not be released.

With all the sensing and actuation elements in place, we turned our attention to the control scheme (Supporting Information Table S3). CNC XYZ translation was serially con-

Research Article
doi.org/10.1002/cmtd.202300043
Chemistry Europe
European Chemical Societies Publishing

trolled with onboard Marlin firmware. An Arduino microcontroller was used to PWM regulate the rotation rates of the mechanical stirrer, inlet wash pump, and outlet wash pump. TriContinent C-series syringe pumps and Sentron pH meter were easily integrated using the detailed serial protocol provided by the respective manufacturers. All processes were run serially except washing, where propeller rotation and inlet pump were run concurrently. A photograph of the complete pH bot and video in operation can be found in the Supporting Information, along with a robot assembly guide.

pH Adjustment and Optimisation Workflow

Having described the pH robot's hardware, we now shift our attention to the titration algorithm, summarised in Figure 5. The initial step is a simple check whether we are already within the target pH range. If not, we add a small random volume of acid or base in the required direction. We sample the random addition from a uniform distribution between a lower and upper bound (LB/UB), which are hyperparameters of the method. These should be set according to domain expertise. Here, the LB and UB are 0.5 and 1.0%, respectively, where this is a percentage of the total volume of sample to be titrated, i.e., for 10 mL, the random volume will be sampled between 50 μL and 100 μL. After adding acid/base at any step, we ensure to mix the solution appropriately and allow the pH to reach a steady-state value. We have programmed the robot to detect when the pH value reaches a steady state, defined as a deviation of less than 0.02 pH units over a period of at least 15 seconds, and we dynamically control the mixing time accordingly.

By this point, we have obtained two initial data points to begin applying a data-driven strategy for pH adjustment. We highlight this as the "physics-informed" ML box in Figure 5. We present a detailed discussion on the physical chemistry basis and ML below, but for now, we focus on the operations of the pH robot. The robot continues with iterations of suggested titrant volumes from the ML model until we reach the target pH range. Please note that the suggested titrant volumes are checked against pre-defined lower and upper bounds, LB_{disp}/UB_{disp}. These may be hardware-dependent. For example, the upper bound could be the max capacity of the syringe. In our study, the lower bound was set to the minimum volume that the syringe pumps could accurately dispense, 25 μL. (Despite the syringe pumps being able to dose to the μL, as stated above, this limit is due to the smallest droplet size at the tip of the dosing needles.) At the other limit, 800 μL was used as the upper bound. These are hyperparameters of the method, which can be guided by domain expertise informed through the traditional titration experiments performed in a dropwise fashion or set through minimal trial-and-error for entirely novel formulation systems. We present the link to the GitHub repository hosting the code to run this titration algorithm and pH platform in the materials and methods section below, as well as in the Supporting Information.

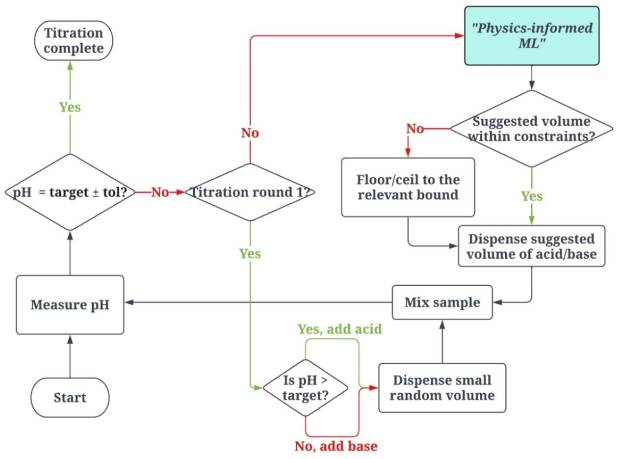

Figure 5. Flowchart of the pH adjustment algorithm for a single sample on the titration robot.

Incorporating Physical Chemistry into the ML Feature Space

We now discuss a key advancement that facilitates the pH robot to titrate with a weak-strong acid/base pair. The amount of protons a weak acid releases into solution is pH-dependent. The analogous argument applies to weak bases. If we take citric acid as H_3A where $A = C_6H_5O_7$ then the effective concentration of protons released into the solution, denoted a_{eff}, is:

$$a_{eff} = (3 \cdot f_{A^{3-}} + 2 \cdot f_{HA^{2-}} + 1 \cdot f_{H_2A^-}) \cdot [H_3A]_0 \quad (1)$$

where $[H_3A]_0 = C_{acid}$ is the concentration of citric acid (M), and f_x is the fraction of the total citric acid present as species x, where citric acid can take up to four speciation states as shown in Figure 1c. However, we are only interested in the three deprotonated states for this tribasic acid. The speciation diagram presented in Figure 1c is calculated through coupling the acid hydrolysis equations with the material balance for the system. This results in the following set of solutions, Equations 2-8. The set of equations is general for any weak, tribasic acid. Derivations for mono/dibasic acids or weak bases are shown in the Supporting Information.

$$H_3A + H_2O \rightleftharpoons H_2A^- + H_3O^+ \quad K_{a1} = \frac{[H_3O^+][H_2A^-]}{[H_3A]} \quad (2)$$

$$H_2A^- + H_2O \rightleftharpoons HA^{2-} + H_3O^+ \quad K_{a2} = \frac{[H_3O^+][HA^{2-}]}{[H_2A^-]} \quad (3)$$

$$HA^{2-} + H_2O \rightleftharpoons A^{3-} + H_3O^+ \quad K_{a3} = \frac{[H_3O^+][A^{3-}]}{[HA^{2-}]} \quad (4)$$

$$[H_3A]_0 = [H_3A] + [H_2A^-] + [HA^{2-}] + [A^{3-}] \quad (5)$$

$$f_{A^{3-}} = \frac{[A^{3-}]}{[H_3A]_0} = \frac{K_{a1}K_{a2}K_{a3}}{[H_3O^+]^3 + K_{a1}[H_3O^+]^2 + K_{a1}K_{a2}[H_3O^+] + K_{a1}K_{a2}K_{a3}} \quad (6)$$

Research Article
doi.org/10.1002/cmtd.202300043
Chemistry Europe
European Chemical Societies Publishing

$$f_{HA^{2-}} = \frac{[HA^{2-}]}{[H_3A]_0} = \frac{K_{a1}K_{a2}[H_3O^+]}{[H_3O^+]^3 + K_{a1}[H_3O^+]^2 + K_{a1}K_{a2}[H_3O^+] + K_{a1}K_{a2}K_{a3}} \quad (7)$$

$$f_{H_2A^-} = \frac{[H_2A^-]}{[H_3A]_0} = \frac{K_{a1}[H_3O^+]^2}{[H_3O^+]^3 + K_{a1}[H_3O^+]^2 + K_{a1}K_{a2}[H_3O^+] + K_{a1}K_{a2}K_{a3}} \quad (8)$$

K_a values are tabulated for a wide range of acids. Using a_{eff}, we calculate the addition of H_3O^+ (moles) as $a_{eff} \cdot V_{acid}$. In this study, we use sodium hydroxide, which is a strong base (full dissociation). Hence the addition of OH^- ions equals $b_{eff} \cdot V_{base}$ where $b_{eff} = C_{NaOH}$ is the concentration of NaOH. Please note, V_{acid}/V_{base} refer to the volume of acid/base, respectively. We train the ML models on net moles, as opposed to net volume, because moles gives a more generalised representation, whereas the titration curve of pH – volume is dependent on concentration. Our ML-driven algorithm works in different stages, which we now detail.

Weighted Initial Sampling

With only two data points, fitting any function more complex than a linear regressor is not meaningful. We fit this model, as demonstrated in Figure 6a, extrapolated between the y-limits of pH 1 to 14. The target pH is represented by the dashed red line in Figure 6a, and we can read off the net moles of H_3O^+/OH^- required to reach the set point. This extrapolation aids us in calculating the quantity of acid/base to be dispensed in the subsequent step. However, early experiments showed, and as can be reasoned through a simple thought experiment: A titration curve typically has a sigmoidal shape. If the initially measured pH points are at either end of the titration curve, then the linear extrapolation will be a significant overestimate of the amount of acid or base required to reach the target pH, as some section of the titration curve will show a steep drop off. This overestimation could lead to an overshoot, consequently forming a complex buffer system. To counter this, we employ a dampening function, depicted in Figure 6b. The range of the dampening function is [0, ζ] where ζ, the dampening constant, is strictly$\leq$1. We used a default value of $\zeta = 0.7$ where lower values of ζ will make the pH adjustment more conservative and therefore, less prone to overshooting. However, too low a value and this will also increase the total time/number of iterations, as the algorithm will take a more incremental step. The maximum of the dampening function, ζ, is found at the pH of the equivalence point between the titrant pair (here we use the third pKa value of citric acid with NaOH as this corresponds to the steep section of citric acid – NaOH titration curve) and the dampening function passes through 0 at pH 0 and 14. We developed the form of the dampening function through fitting a rational function approximation and details for this and computing the equivalence point of a weak-strong acid/base system, are in the Supporting Information. If we have a strong-strong acid/base pair then their equivalence point will be at pH 7 and a simpler polynomial fit can be used for the dampening function, again obeying the same properties as outlined above. We utilise the mid-point pH of the initial two data points to derive the weight, w, from the dampening function. Then, we multiply the extrapolated volume to be added by w to suggest the titrant volume for the second step. We have once again employed our physical understanding of the system to design the titration algorithm.

Titrating Formulations via Physics-informed Bayesian Optimisation

After we have at least three data points, we are able to fit a Gaussian Process (GP) surrogate model over the titration curve. This is one of the very few models shown to work in a very-low data regime[27] and was the best-performing model in our group's past study.[13] GPs are the workhorse of Bayesian Optimisation (BO), an algorithm used to optimise a black-box function, $f(x)$, which is expensive to evaluate.[28,29] Here we could think of minimising $f(net\ moles) = |titration\ curve(net\ moles) - pH_{target}|$. The basic recipe for BO is a surrogate model trained over an initial dataset. After this, a cheaper-to-evaluate (than the original $f(x)$) acquisition function, $\alpha(x)$, is evaluated by querying the

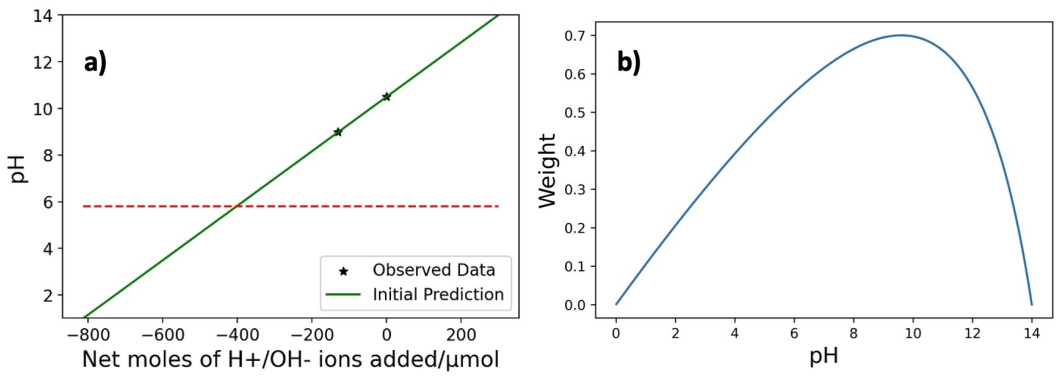

Figure 6. Weighted linear model: a) Linear spline extrapolation is used to determine the next (2nd) step in the experiment; b) A pH-dependent dampening function is used to modulate the suggested step from the linear model to reduce the probability of overshooting the target pH (red dashed line).

Research Article
doi.org/10.1002/cmtd.202300043
Chemistry Europe
European Chemical Societies Publishing

surrogate model and used to suggest the next sample. The dataset is updated, and the cycle is repeated until a termination condition is reached. In this case, this is done until we are within the target pH range, as shown in Figure 5. Here, the simplest form of the acquisition form, $\alpha(x)$, probability of improvement (PI) is selected, as this acquisition function is completely exploitative, and we are trying to reach the pH target in the fewest iterations. Typically, expected improvement (EI), which balances exploration and exploitation is preferred as PI assigns a reward regardless of the magnitude of improvement. This can result in getting stuck in local optima.[30] However, we select PI knowing that there are no local minima to be concerned about due to smooth, monotone nature of a titration curve. This knowledge also helps guide our choice of GP kernel. A radial basis function (RBF) kernel is selected due to its smooth properties.[31] And finally, we reformulate the surrogate model due to the titration curve's monotonicity. Typically, a GP has its mean function set to zero, as if no better prior is known and the data is pre-processed via standardisation, then this is a good starting point.[27] However, informed by the physics of the system, we wish to model a GP with a linear and monotonically increasing mean function. We achieve this through fitting a linear regressor over the experimental data points and then a GP (with zero mean) is fit to the errors between the linear regressor's predictions and the experimental data points. No pre-processing is required on the data, meaning we can directly train the model on the same scale that the experimentalist is working in. This is equivalent to having a GP with a linear and monotonically increasing mean function and produces the desired model fits, as illustrated in Figure 7. The scikit-learn implementation of the RBF kernel has a single hyperparameter to be tuned, the horizontal length scale, which controls the periodicity of the fitting function. Finally, to re-emphasise, these ML models are being trained on a feature space, net moles, which is being calculated via a physical model. The results in Figure 7 (and later in Figure 9 too) show that few iterations are required to reach the target pH and highlight the benefit of using such a "physics-informed" approach.

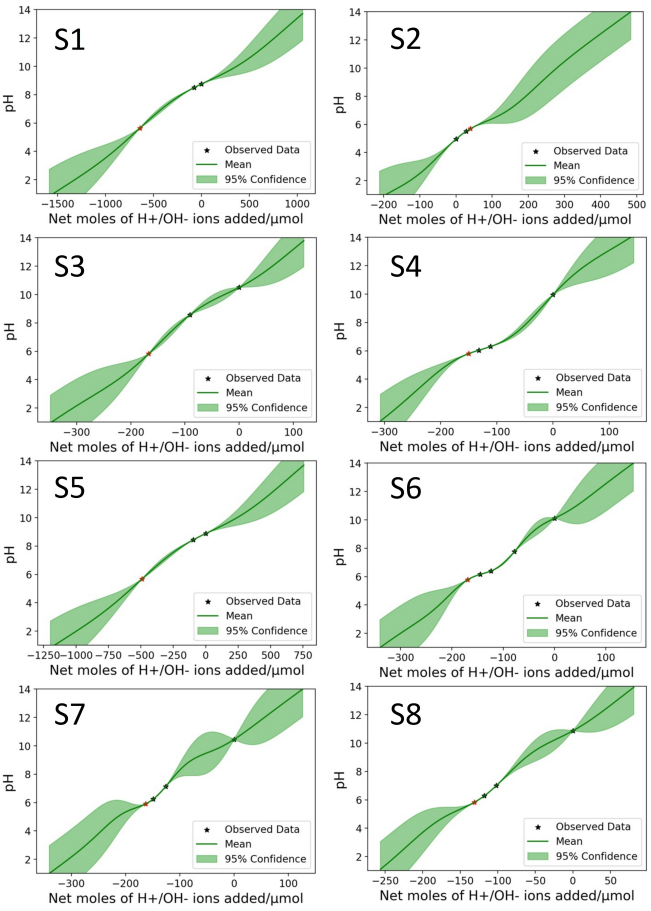

Figure 7. Gaussian Process surrogate models over the titration curves of eight formulation samples used in a Bayesian Optimisation framework to adjust the samples to pH 5.8±0.2.

Compensating for a Buffer System if the pH Target is Overshot

The GP model is used till the target pH is reached or an overshoot occurs. If the algorithm overshoots the target, in making a correction, a complex buffer system, resistant to pH change, will be formed. In this case, we pivot to an alternative strategy, given by Equation (9), based on estimating the sample's "buffer capacity" (β).

$$V = \mu \times \beta \times \left(pH_{current} - pH_{target}\right) \text{ where } \beta = \frac{\Delta V}{\Delta pH} \tag{9}$$

Here μ is a different dampening parameter to before and we have set μ as 0.7 based on trial-and-error experiments. This is a good default for our formulations: we hypothesise that a highly sensitive buffer system would require a stronger dampening (lower μ). We use the above equation to calculate the next suggested titrant volume when in the overshoot region. Please see the Supporting Information for a sample calculation.

If we did not follow such an alternative method, we would experience significant complications. The sample shown in Figure 8 involves titrating a formulation to pH 6 using a purely Bayesian approach, similar to the method of Pomberger et al.,[13] i.e., without an option for a different overshoot strategy. The initialisation procedure is the same as presented above. The sample starts at a high pH > 12 and upon a small random addition of acid (here = 55 μL), the pH does not decrease much. Therefore, at the next step, the model thinks it needs to add lots of acid. Here a constraint is activated, and in this case, an upper bound of 1 mL of citric acid is added. This causes the pH to overshoot the set point and drop to close to 4.5. From here on sodium hydroxide is added back as a correction, but the strong base is reacting with the citric acid to convert some of it into its conjugate base and thereby form a citrate buffer system which is making the whole formulation challenging to titrate. In reality, a buffer system so resistant to pH change is formed, that more than 1 mL of base needs to be added back and we would not return to our starting pH; however, the Bayesian method

Research Article
doi.org/10.1002/cmtd.202300043
Chemistry Europe
European Chemical Societies Publishing

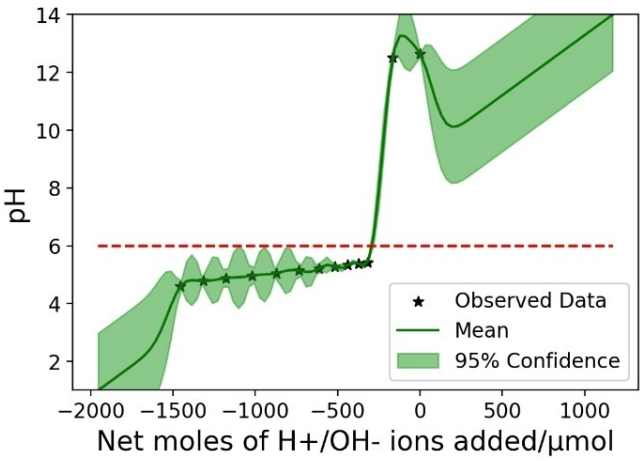

Figure 8. Pitfalls of a purely Bayesian approach when a pH adjustment overshoots.

does not know this. The surrogate model still thinks that at $-55\,\mu L$ the pH will be ~12 and so we see it takes several iterations (12 are presented in Figure 8) where the suggested experiments creep back to the starting point. However, the model cannot go there as it falsely predicts an almost instantaneous jump to the pH point from the initialisation. The model is not smart. In fact, this experiment continued for a further 4 iterations until the GP was unable to model the discontinuous jump and finally failed after 16 iterations.

Therefore, upon observing this behaviour with early iterations of the algorithm, we modified the method to detect when we are in the overshoot region. This is defined by the addition of acid, followed by base or vice versa, i.e., when a correction is used and therefore going to form a complex buffer. Following this, Equation (9) presented above is used, only looking at the past two data points and not the full history, to adjust the sample. The algorithm works such that an overshoot is corrected regardless of which direction you approach the titration curve from and also in the very worst-case scenario, if the overshoot occurs again, then the sample can still be recovered. All in all, it is important to consider the complication which arises from using a weak-strong acid/base pair for the titration and a combined physics-informed ML method works effectively here, whereas a black-box, purely exploitative Bayesian Optimiser without knowledge of the chemistry fails.

Performance of the Titration Algorithm

We developed and are actively using the titration robot as part of a wider project on liquid formulations. We are generating a high-throughput dataset, for which the pH adjustment process is a crucial step of the workflow and our industrial partner specified that all products must be pH 5.8±0.2. Figure 9a shows the number of iterations required to titrate over 250 viscous formulations which have been adjusted on the pH platform to date. These formulations took on average 15 minutes per sample for pH adjustment, including cleaning. The physics-informed pH optimisation, coupled with an automated titration and cleaning robot is critical to enable such a high-throughput, previously not possible as these titrations are typically a lengthy manual affair. Furthermore, as shown by Figure 9b, we are able to titrate formulations spanning the full pH spectrum. While all our products are titrated to the same narrow pH range, the pHbot and titration algorithm are flexible to adjust samples to any specified set point. The only caveat is to ensure that the acid and base selected are suited for a given titration target. For example, if the pH target is close to a particular titrant pair's equivalence point, then the titration will be more challenging, and it is recommended an alternative acid or base is selected. The algorithm however only requires the acid (or base) hydrolysis constant(s) for the titrant, and as demonstrated on the web application introduced below, is flexible to work with any strong-strong or weak-strong acid-base pairs and we can therefore access any target pH range.

We demonstrate that the algorithm is efficient as the majority of samples are titrated without overshoot and these samples typically required between only two to four iterations on our pH robot. This is on par if not more efficient and generally applicable than the method presented in[13] despite working with a more complex titration as we are using citric acid (a weak, polyprotic titrant) and do not feed the method

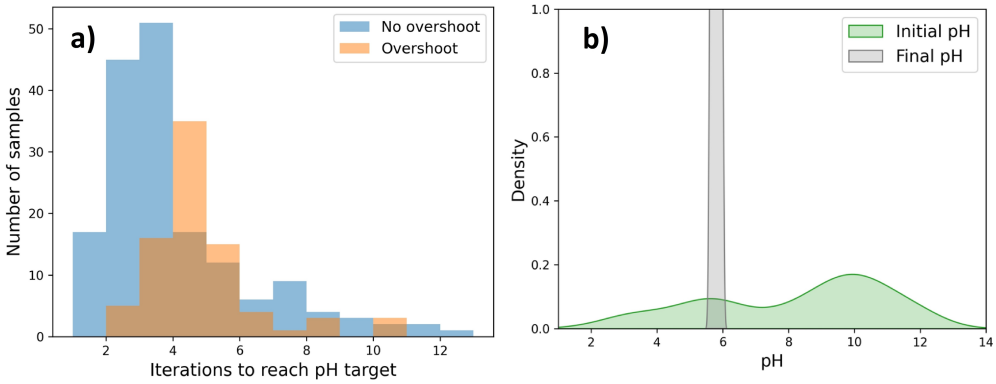

Figure 9. Evaluation of titration algorithm: a) Performance across 250 + formulation samples; b) Density distribution of the initial and final pH values for the tested formulations.

any information about the system being adjusted. This validates the developments made to our titration algorithm, such as modelling the GP with a linear and monotonically increasing mean function. As expected, the distribution for the overshot samples lies to the right of those that do not overshoot. Here, the mode number of iterations to reach the target pH is five. This is quite reasonable considering the complexity of adjusting a system with a citrate buffer. Additionally, we see the overall distribution is positively skewed with some particularly difficult samples. These were samples which themselves contained ingredients with a buffering agent. Overall, though, the algorithm works efficiently and the rate limiting step for the overall pH adjustment is the mixing time after acid or base addition. As mentioned above, we have optimised this through implementing dynamic control of the mixing time; we only stir the formulations for as long as it takes their pH to reach steady state (measured via continuous logging of the pH meter). Therefore, the titration process is as efficient as it can be.

Titration Algorithm Web Application

We provide full details and links in the Supporting Information to build this pH robot. There is a main code, which calls object-oriented methods to control the hardware, that also includes the titration algorithm. The Jupyter Notebook via which the pH robot is run is relatively easy to use, however, we wished to decouple the titration algorithm from the robot, so that we can encourage a wider audience to use the "physics-informed" ML method without going to the efforts of reproducing the hardware. Therefore, a web application has been developed on Streamlit (https://aniketchitre-accelerate-titrations-titrationalgo-webapp-z383g2.streamlit.app/) as a front-end to the titration algorithm. The code has been generalised to work with different acids/bases and sample volumes to accelerate a variety of titration tasks, as the general equations presented in the Supporting Information are encoded into the web application. Other acids/bases can be added upon request.

Scale-up Studies

We prepared six formulations up to 250 mL, a scale-up factor x25 in volume vs. the experiments conducted on the pH robot. This is closer to industrial formulation development tasks. We adjusted the formulations to pH 5.8±0.2 using 0.5 M citric acid/0.5 M sodium hydroxide following the suggestions from the titration algorithm web application. Table 1 presents the results of these titrations. The scale-up experiments were carried out as a bench-top titration, similar to traditional pH adjustment experiments in industrial research and development (R&D) laboratories. The setup is detailed in the materials and methods section. These experiments were conducted to: (i) demonstrate the scale-invariance of the algorithm and its application to accelerate traditional benchtop titrations; (ii) investigate the role of viscosity for optimising mixing.

On average, the titrations were completed in just three iterations as indicated in Table 1, where the samples are labelled as SU-# (with SU representing scale-up and # representing the sample number). This constitutes an initialisation of two data points + one suggestion from the GP surrogate model, which highlights the potential of the titration algorithm to accelerate traditional pH adjustment workflows. We see that the algorithm overshoots the set-point for SU-1 and SU-6 (one third of the total samples tested), which is roughly consistent with the results presented in Figure 9 – but is able to successfully reach the end point despite the formation of a complex citrate buffer system. The formulations start out predominantly basic, but the algorithm is able to adjust formulations from either side of the set-point, for example, SU-6 starts out acidic.

We performed the scaled-up experiments in a 500 mL beaker with a high torque stirrer – effectively a stirrer tank – and the pH of the formulation was continuously logged upon addition of acid or base, until it stabilised. See the materials and methods for details. We additionally note, as shown from Table S4 (Supporting Information), that the optimal mixing time, i.e., the shortest time for the pH to stabilise, changed upon each iteration of the titration for some formulations. As supported by Figure S5 this is because viscosity of the formulations has a pH dependency. Since the formulation's rheology was only characterised for the final sample product, the time for pH stabilisation on the last iteration of pH adjustment is taken and plotted against the formulation's apparent viscosity (taken as the viscosity at a shear rate of 10 s^{-1}) in Figure 10. Apparent viscosity is used here, as the formulations are non-Newtonian, however this is referred to simply as viscosity from here on. A linear best fit line on a log-log plot shows us a power law relationship, supported with a high R^2 value of 0.92 that the optimal mixing time, t, is $\propto \eta^a$ where η is the viscosity and a is some fixed exponent. The

Table 1. Titration results for scaled-up formulation samples (250 mL) adjusted to pH 5.8±0.2 using the titration algorithm's suggestion from the Streamlit web application.

	SU-1		SU-2		SU-3		SU-4		SU-5		SU-6	
Step	Net V (mL)	pH	Net V (mL)	pH	Net V (mL)	pH	Net V (mL)	pH	Net V (mL)	pH	Net V (mL)	pH
0	0	10.23	0	10.52	0	8.63	0	8.90	0	11.75	0	4.84
1	−1.4	8.51	−2.1	8.18	−1.9	8.30	−2.0	8.26	−1.7	11.10	+1.9	5.11
2	−3.5	5.39	−4.1	**5.89**	−9.9	6.79	−9.1	6.47	−9.7	5.20	+4.0	5.50
3	−3.2	**5.67**			−14.9	**5.71**	−12.2	**5.66**	−8.6	5.33	+5.4	**5.95**
4									−5.8	**5.65**		

Research Article
doi.org/10.1002/cmtd.202300043
Chemistry Europe
European Chemical Societies Publishing

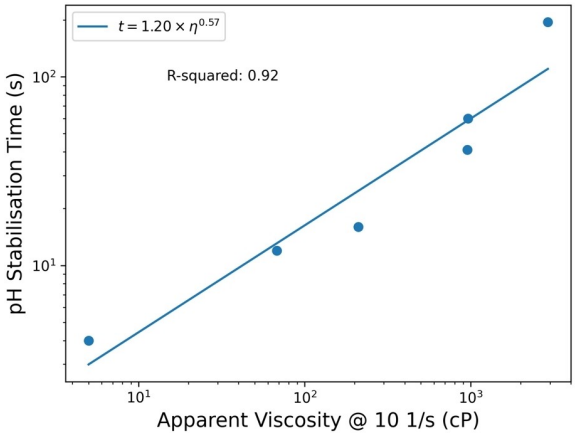

Figure 10. The optimal mixing time for viscous formulations in a stirred tank approximately follows a power-law relationship with the sample's viscosity.

power-law relationship for the particular set-up used is shown in the legend of Figure 10, however, this is dependent on the dimensions of the stirred tank and speed of the stirrer. The general observation, however, is of greater significance, and guided us to implement dynamic control of mixing time on the pH robot. We were previously mixing all the formulations for 'as long as required' to homogenise the most viscous samples in the experimental set, where in fact the less viscous formulations could be well mixed much more quickly thereby reducing the experimental time further.

Conclusions

We have developed a self-driving pH robot to autonomously perform small scale batch titration of viscous liquid formulations, which is a challenging, yet common industrial task. This titration is often carried out using a weak, polyprotic titrant, namely, citric acid as it confers certain benefits to the final formulation. This necessitated the advancement of a machine-learning driven titration algorithm to incorporate a physical chemistry model for the weak titrant's pH-dependent speciation state. The final presented pH adjustment strategy is a multi-stage algorithm capable of adjusting a wide variety of systems using any combination of strong-strong or weak-strong acid/base pairs. The method is able to recover and successfully titrate even those samples which have overshot the set point and therefore resulted in the formation of a potentially complex buffer system in solution. Across a range of over 250 samples, it typically took two to five iterations to converge on the pH target. The titration algorithm is run onboard the pH robot, resulting in the platform's self-driving capability, and has additionally been shared as a standalone user-friendly web application. This web application was utilised to successfully drive the pH adjustment of scaled up formulation samples, closer to industrial R&D volumes, within an average of just three iterations. Finally, a power-law relationship was experimentally defined between the optimal mixing time after acid/base addition and the formulation's viscosity. Overall, a "physics-informed" ML method and titration robot have been presented to accelerate industrially-relevant pH adjustment workflows.

Experimental Section

The presented pH robot was designed and developed in-house. An assembly guided is provided in the Supporting Information. A bill of materials (Table S1) for commercially purchased parts and 3d-printed parts (Table S2) can be found in the Supporting Information. Additionally, the CAD design files to 3d-print the parts can be found under the following GitHub repository: https://github.com/sustainable-processes/pHbot. This repository has the codes for the equipment firmware, as well as a main Jupyter Notebook to operate and run the pH robot, including the titration algorithm.

Preparation of Liquid Formulations

The liquid formulations were prepared into 15 g cosmetic jars purchased from the CJT Store on AliExpress. The formulations were prepared using a binary mixture of surfactants, a conditioning polymer and a thickener in a base of water. The following wide range of commercial ingredients were used as received from BASF: (i) surfactants: Texapon SB 3 KC, Plantapon ACG 50, Plantapon LC 7, Plantacare 818, Plantacare 2000, Dehyton MC, Dehyton PK 45, Dehyton ML, Dehyton AB 30, Plantapon Amino SCG-L, Plantapon Amino KG-L, Dehyquart A-CA; (ii) polymers: Luviquat Excellence, Dehyquart CC6, Dehyquart CC7 Benz, Salcare Super 7; (iii) thickeners: Arlypon TT, Arlypon F. These ingredients were pipetted into the cosmetic jars using a retrofitted Opentrons OT-2 liquid handling robot. Then the formulations were mixed for 35 minutes at 360 rpm at 25 °C using FischerBrand rare earth octagonal stir bars (25×8 mm). Only stable formulations, i.e., those appearing as a visually homogenous phase, were tested on the pH robot. Additionally, commercial shampoo products from Head & Shoulders and Sunsilk, were tested too.

pH Probe Calibration and Preparation of Acid/Base Stock Solutions

The Sentron MicroFET pH probe was calibrated daily with a 3-point calibration at pH 4, 7, 10 using original Sentron buffer solutions (pH 4: A116-004, pH 7: A116-007, pH 10: A116-10). These are N.I.S.T based, high quality reference fluids. Acid and base stock solutions were prepared up to the required concentration, typically 0.5 M throughout this study, using citric acid (CAS 77–92-9; ACS reagent, $\geq$99.5 %) and sodium hydroxide (CAS 1310–73-2; reagent grade, $\geq$98 %, pellets (anhydrous)) purchased from Sigma Aldirch.

Scale-up Studies

Figure S4 shows the set-up for the scaled-up experiment, a bench-top titration. 250 mL of formulation sample was prepared up on a balance in a 500 mL glass beaker. This was then placed underneath a FischerBrand™ Universal Overhead Stirrer with a crossed blade impeller, which was operated at 300 rpm with a clearance from the bottom around 2.5 cm. The Sentron MicroFET probe (connected to the SI 600 pH meter), was held in place by a clamp stand and immersed to a depth of approximately 2 cm into the bulk formulation fluid. The pH meter was connected to a laptop to digitally log the data. 0.5 M citric acid and 0.5 M sodium hydroxide stock solutions were used for the pH adjustment, which were dosed manually following the suggestion of the titration algorithm on the Streamlit web application. It is detailed in the Supporting

Information how the pH stabilisation time was recorded. Finally, we measured the rheology of the samples on a TA Instruments DHR 30 rheometer at 25 °C with a 60 mm stainless steel parallel plate using a 250 μm geometery gap. A shear rate sweep between 1–1000 s^{-1} was performed.

Acknowledgements

This project was co-funded by the Accelerated Materials Development for Manufacturing Program at A*STAR via the AME Programmatic Fund by the Agency for Science, Technology and Research under Grant No. A1898b0043, and the National Research Foundation (NRF), Prime Minister's Office, Singapore under its Campus for Research Excellence and Technological Enterprise (CREATE) program as a part of the Cambridge Centre for Advanced Research and Education in Singapore Ltd (CARES). A.C. is grateful to BASF for co-funding his PhD. The authors would like to thank Dr Antonio Del Rio Chanona for suggesting an implementation of a monotonically increasing Gaussian Process surrogate model, and Prof. Ian Wilson for a helpful discussion on the cleaning protocol. And finally, to acknowledge Leong Chang Jie for re-purposing his control code of the Ender platform in our work.

Conflict of Interests

The authors declare no conflict of interest.

Data Availability Statement

The data that support the findings of this study are available in the supplementary material of this article.

Keywords: Formulations · Hybrid model · Machine learning · Robotics · Titration

[1] M. Lukić, I. Pantelić, S. D. Savić, *Cosmetics* **2021**, *8*, 1–18.
[2] S. Hawkins, B. R. Dasgupta, K. P. Ananthapadmanabhan, *Intern J of Cosmetic Sci* **2021**, *43*, 474–483.
[3] J. J. Griffin, R. F. Corcoran, K. K. Akana, *J. Chem. Educ.* **1977**, *54*, 553–554.
[4] M. F. Gavazzoni Dias, J. Pichler, A. Adriano, P. Cecato, A. De Almeida, *Int J Trichol* **2014**, *6*, 95–99.
[5] S. Vázquez-Blanco, L. González-Freire, M. C. Dávila-Pousa, C. Crespo-Diz, *Farm. Hosp.* **2018**, *42*, 221–227.
[6] I. Sodini, J. Mattas, P. S. Tong, *Int. Dairy J.* **2006**, *16*, 1464–1469.
[7] R. E. Anli, Ö. A. Cavuldak, *J. Inst. Brew.* **2012**, *118*, 368–385.
[8] R. Lopez-Garcia, *Kirk-Othmer Encyclopedia of Chemical Technology*, John Wiley & Sons, Inc., Hoboken, NJ, USA, **2010**, pp. 1–25.
[9] S. Nangare, Y. Vispute, R. Tade, S. Dugam, P. Patil, *Futur J Pharm Sci* **2021**, *7*, 1–23.
[10] L. Cao, D. Russo, K. Felton, D. Salley, A. Sharma, G. Keenan, W. Mauer, H. Gao, L. Cronin, A. A. Lapkin, *Cell Rep. Phys. Sci.* **2021**, *2*, 100295.
[11] H. N. Po, N. M. Senozan, *J. Chem. Educ.* **2001**, *78*, 1499–1503.
[12] M. K. Nguyen, L. Kao, I. Kurtz, *Am. J. Physiol.* **2009**, *296*, F1521–F1529.
[13] A. Pomberger, N. Jose, D. Walz, J. Meissner, C. Holze, M. Kopczynski, P. Müller-Bischof, A. A. Lapkin, *Chem. Eng. J.* **2023**, *451*, 139099.
[14] J. L. McDonagh, W. C. Swope, R. L. Anderson, M. A. Johnston, D. J. Bray, *Polym. Int.* **2021**, *70*, 1–8.
[15] V. Venkatasubramanian, *AIChE J.* **2019**, *65*, 466–478.
[16] M. Ulbrich, V. Aggarwal, *J. Bus. Chem.* **2019**, *2*, 76–81.
[17] C. J. Leong, K. Y. A. Low, J. Recatala-Gomez, P. Q. Velasco, E. Vissol-Gaudin, J. D. Tan, B. Ramalingam, R. I. Made, S. Dinesh, S. Sebastian, Y.-F. Lim, Z. H. J. Khoo, Y. Bai, J. J. Cheng, K. Hippalgaonkar, *Matter* **2022**, *5*, 3124–3134.
[18] D. C. Harris, *Quantitative Chemical Analysis*, 8th Edition, W. H Freeman & Co Ltd., New York, NY, USA, **2010**, 22–25.
[19] J. Tyson, *Anal. Proc.* **1987**, *1*, 1358.
[20] K. K. Stewart, A. G. Rosenfeld, *J. Autom. Chem.* **1981**, *3*, 30–32.
[21] J. Kozak, J. Paluch, M. Kozak, M. Duracz, M. Wieczorek, P. Kościelniak, *Molecules* **2020**, *25*, 1533.
[22] E. V. Aquino, C. Pasquini, J. J. R. Rohwedder, I. M. Raimundo Jr, M. C. B. S. M. Montenegro, A. N. Araújo, *J. Braz. Chem. Soc.* **2004**, *15*, 111–115.
[23] M. Christensen, L. P. E. Yunker, P. Shiri, T. Zepel, P. L. Prieto, S. Grunert, F. Bork, J. E. Hein, *Chem. Sci.* **2021**, *12*, 15473–15490.
[24] H. Fleischer, K. Thurow, *Automation Solutions for Analytical Measurements: Concepts and Applications*, Wiley-VCH, Hoboken, NJ, USA, **2017**.
[25] E. Vorberg, PhD thesis, University of Rostock (Germany), **2015**, p. 23..
[26] K. Werner, *Handbook of Semiconductor Wafer Cleaning Technology - Science, Technology, and Applications*, 1st Edition, William Andrew Publishing, Norwich, NY, USA, **1993**, p. 121.
[27] R.-R. Griffiths, *PhD thesis*, University of Cambridge (UK), **2022**, pp 13-28.
[28] B. Shahriari, K. Swersky, Z. Wang, R. P. Adams, N. de Freitas, *Proc. IEEE* **2016**, *104*, 148–175.
[29] S. Greenhill, S. Rana, S. Gupta, P. Vellanki, S. Venkatesh, *IEEE Access* **2020**, *8*, 13937–13948.
[30] R. Garnett, "Bayesian Optimisation", can be found at https://www.cse.wustl.edu/~garnett/cse515t/spring_2015/files/lecture notes/12.pdf, **2015** (accessed 30 April 2023).
[31] D. K. Duvenaud, *PhD thesis*, University of Cambridge (UK), **2014**, pp. 9-10.

Manuscript received: August 23, 2023
Version of record online: December 13, 2023